[5]A. Goldberg, H. M. Schey, and J. L. Schwartz, "Computer-generated motion pictures of one-dimensional quantum-mechanical transmission and reflection phenomena," Am. J. Phys. **35**, 177–186 (1967); "One-dimensional scattering in configuration space and momentum space," *ibid.* **36**, 454–455 (1968).
[6]M. H. Bramball and B. M. Casper, "Reflections on a wave packet approach to quantum mechanical barrier penetration," Am. J. Phys. **38**, 1136–1145 (1970).
[7]J. R. Merrill, "The propagation of quantum mechanical wave packets," Am. J. Phys. **41**, 1101–1103 (1973).
[8]J. S. Boleman and S. B. Haley, "More time-dependent calculations for the Schrödinger equation," Am. J. Phys. **43**, 270–271 (1975).
[9]C. Segre and J. D. Sullivan, "Bound-state wave packets," Am. J. Phys. **44**, 729–732 (1976).
[10]E. A. Johnson and H. T. Williams, "Quantum solutions for a symmetric double square well," Am. J. Phys. **50**, 239–243 (1982).
[11]I. Galbraith, Y. S. Ching, and E. Abraham, "Two-dimensional time-dependent quantum-mechanical scattering event," Am. J. Phys. **52**, 60–68 (1983).
[12]See, e.g., Ref. 1, pp. 192–195.
[13]The momentum-space wave functions for scattering are briefly discussed and illustrated in the second reference of Ref. 5.
[14]A. Goswami, *Quantum Mechanics* (Brown, Dubuque, 1992), pp. 88–91.
[15]R. Winter, *Quantum Physics* (Wadsworth, Belmont, 1979), pp. 92–97.
[16]S. Wolfram, *Mathematica: A System for Doing Mathematics by Computer* (Addison-Wesley, Reading, MA, 1991).
[17]M. Abramowitz and I. A. Stegun, *Handbook of Mathematical Functions* (National Bureau of Standards, Washington, D.C., 1964), pp. 446–449.
[18]D. Park, *Introduction to the Quantum Theory* (McGraw-Hill, New York, 1992), 3rd ed., pp. 106–109.
[19]B. Holstein, *Topics in Advanced Quantum Mechanics* (Addison-Wesley, Reading, MA, 1992), pp. 108–110.

Control of the chaotic driven pendulum

Gregory L. Baker
College of the Academy of the New Church, Bryn Athyn, Pennsylvania 19009

(Received 23 March 1994; accepted 21 December 1994)

A method of controlling chaos (due to Ott, Grebogi, and Yorke) is illustrated with a simulated chaotic pendulum. The method consists of stabilizing a previously unstable periodic orbit through a feedback mechanism that periodically adjusts the damping parameter of the pendulum. The presentation is pedagogical and describes the method in more detail than is typical of the research literature on controlling chaotic systems. © *1995 American Association of Physics Teachers.*

I. INTRODUCTION

The pendulum has long served as a pedagogically useful model in mechanics. From Galileo's discovery of the approximate constancy of its period for small oscillations,[1] to its recent use as an experimental[2] and simulation model[3,4] for nonlinear dynamics, the pendulum has exhibited a rich variety of dynamical behavior. The pendulum has for many decades exemplified periodic motion,[5] and its more recent emergence as a primary example of chaotic dynamics has made it ubiquitous in the mushrooming pedagogical literature on chaotic dynamics.[3,6,7] In this paper we use the pendulum to illustrate the "control of chaos."

The control of physical systems is an important subject in engineering, and the classical literature is extensive.[8] However the application of control algorithms to chaotic dynamics is recent. The goal is to continually but slightly perturb a chaotic mechanical system so as to cause it to act nonchaotically. More precisely, the parameters of the system are such that it would ordinarily exhibit chaos and yet the system can be made to behave periodically by a time-varying adjustment of the parameters *in the chaotic range*. The requisite size of the perturbation depends on the momentary deviation from periodicity, and therefore the control mechanism is a version of proportional feedback.

This and other similar control algorithms may have important application in a variety of areas where chaotic signals are present.[9] Typical examples include possible control of cardiac fibrillation, epileptic seizures, and chemical reactions.[10] Control may also be used to extend the stability regime of lasers[11] and has even been suggested as a strategy for efficient vaccination of populations against various diseases.[12]

While several control mechanisms for chaotic systems are known, we confine our discussion to the elegant scheme proposed by Ott, Grebogi, and Yorke[13] (OGY) in 1990 and very quickly applied to a physical system, the magnetoelastic ribbon, by Ditto, Rauseo, and Spano.[9,14] Variations of the OGY scheme have been applied to other oscillating systems. For example, control of a "parametric" pendulum—one whose pivot point is driven vertically—has been achieved both in experiment and numerical simulation by Starrett and Tagg.[15] Nitsche and Dressler have achieved control when the dynamical system is known only by a time series. They applied their modification of OGY control to a time series from a simulated Duffing oscillator.[16] Finally, Hubinger, Doerner, and Martiennsen[17] used an extension of the OGY method (involving quasicontinuous control) to control an experimental pendulum.

In the original paper the OGY method was applied to the two-dimensional Henon map. Here we take a similar approach and use the Poincaré section of the forced, damped pendulum as a two-dimensional map.

We begin with a brief description of the simulated driven pendulum. Then two representations of chaotic behavior are described: (1) a *bifurcation diagram* which displays dynamical behavior over a range of control parameter values, and (2) a *Poincaré section* which shows periodic sampling of the state variables, angle θ_n, and angular velocity ω_n. Finally, the OGY algorithm is applied to the pendulum—in part, to

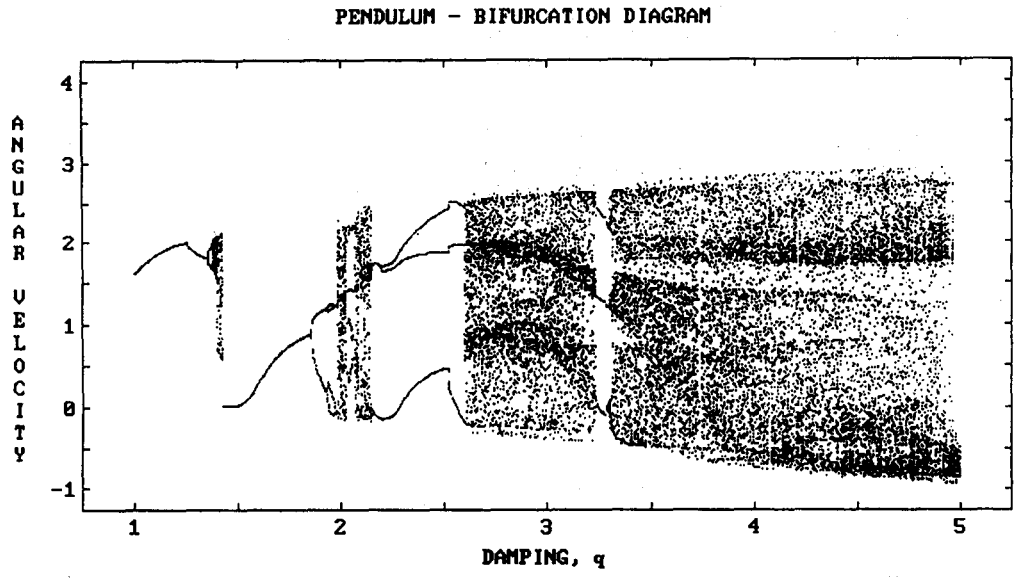

Fig. 1. A bifurcation diagram for the driven pendulum. The angular velocity ω of the pendulum at the beginning of each forcing cycle is plotted for many cycles at each value of the friction parameter q. In regions where there are many values of angular velocity, the motion is chaotic. The forcing parameter is $g=1.5$ and the forcing frequency $\omega_D=2/3$.

encourage the nonspecialist to experiment with the control of chaos with pendula and other periodically forced chaotic systems.

II. THE CHAOTIC PENDULUM

The chaotic pendulum is a driven pendulum that is operated in a parameter regime where the motion is chaotic. In dimensionless form its equation of motion may be written as

$$\frac{d^2\theta}{dt^2}+\frac{1}{q}\frac{d\theta}{dt}+\sin\theta=g\cos\omega_D t, \tag{1}$$

where θ is the angular displacement of the pendulum from the vertical, q is a friction parameter, g is the forcing amplitude, and ω_D is the forcing frequency.[3] (Small values of q imply large damping.) Variation of the parameter set (q,g,ω_D) results in various types of dynamical behavior, including chaos. The *bifurcation diagram* of Fig. 1 illustrates some of this variety. In Fig. 1 the horizontal axis shows the increase in the friction parameter q (actually a decrease in the damping) and the vertical axis shows the value of the angular velocity, $\omega=d\theta/dt$, taken at the beginning of each of many forcing cycles, *after initial transients have died away*. If the motion is periodic at the forcing frequency, then only one point occurs repeatedly for that value of q. If only a few points occur then the motion is periodic with a periodicity indicated by the number of points. For example, a period-3 window occurs at about $q=3.24$. Such periodic orbits are stable motions. If there are many points—a broad spectrum of values of ω—then the motion never repeats and is chaotic. In this case, infinitely many periodic orbits are present, but all are unstable. For this discussion we focus on the dynamics associated with a parameter set $(g=1.5, q=3.9, \omega_D=2/3)$ that lies well inside the chaotic zone, as indicated in the bifurcation diagram.

Another diagram—the *Poincaré section*—is also important for this discussion. The Poincaré section, as seen in Fig. 2, is a stroboscopic picture of the (θ,ω) plane for the pendulum taken once during each forcing cycle after initial transients have died away. In this case the coordinates are measured at the beginning of each forcing cycle and the parameter values used in Fig. 2 are the ones stated above. Because the system is governed by Newton's second law there is a deterministic relationship between successive points that may be represented mathematically as

$$\begin{pmatrix}\theta_{n+1}\\ \omega_{n+1}\end{pmatrix}=m(\theta,\omega)\begin{pmatrix}\theta_n\\ \omega_n\end{pmatrix}, \tag{2}$$

where $m(\theta,\omega)$ is some unknown transformation acting on the vector (θ_n,ω_n) that represents each point. The Poincaré section is therefore a geometric representation of this transformation. For control, it is important to determine m at a certain point in the phase plane.

III. THE OGY METHOD OF CONTROL

The OGY method rests upon the fact that in the chaotic regime there are infinitely many *unstable* periodic orbits.[9] These orbits are represented on the Poincaré section by *fixed points*—points that stay constant from cycle to cycle. Since the periodic orbits are unstable, an actual trajectory will only return to the vicinity of these unstable fixed points a few times. Control is achieved by keeping the system near one of those unstable periodic orbits indefinitely by suitable small changes in a parameter. In this case the friction parameter q is given a small change δq at the beginning of each drive cycle. The amount of change δq is based upon the deviation of the system's trajectory from the periodic orbit. An appropriately chosen value of δq causes the system's trajectory to be pushed back toward the periodic orbit during the subsequent cycle. Repetition of the process "stabilizes" the un-

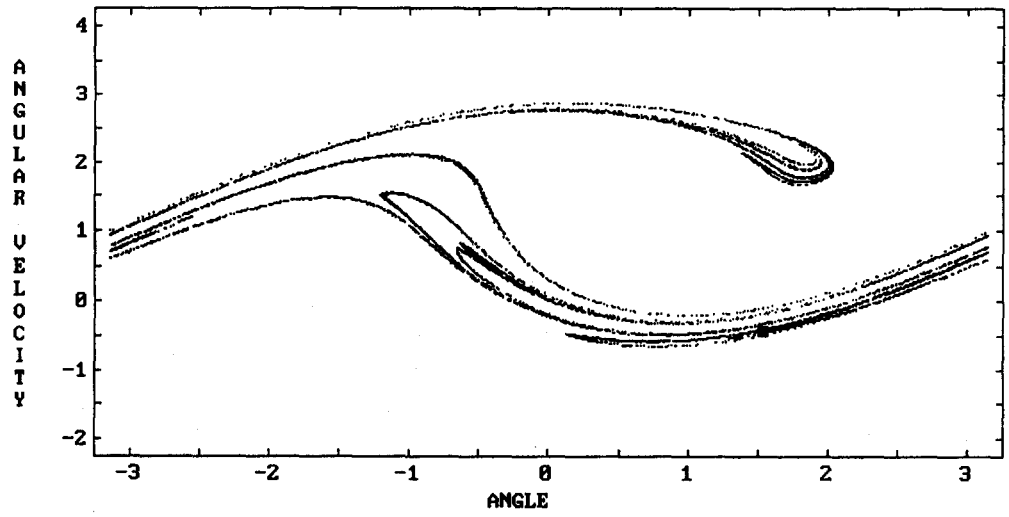

Fig. 2. A Poincaré section for the pendulum when $g=1.5$, $q=3.9$, and $\omega_D=2/3$. The values of angular velocity ω and angle θ are plotted at the beginning of each forcing cycle, for 10 000 cycles. The solid square near (1.5, −0.5) contains an unstable fixed point. (See later text for explanation.)

stable periodic orbit. Unlike some other control methods, the OGY method has the useful feature that it is applicable even when only small changes to the system dynamics are tolerable. In this way the locations in phase space of the fixed points are only slightly affected by the control process, yet the system may operate periodically.
The steps in the method are as follows.

(1) Determine the coordinates of a fixed point (θ_F,ω_F) on the Poincaré section of an unstable periodic orbit.
(2) Determine the effect of small changes in the parameter q on the coordinates of the fixed point.
(3) Determine the transformation m in the region of the fixed point.
(4) Use this information to adjust the parameter change δq so as to force the next trajectory back toward the fixed point on the Poincaré surface of section.

In this way the intersection of the trajectory with the Poincaré section is kept in the region of the fixed point and the pendulum undergoes nearly periodic motion. Let us follow the details of these steps.

A. Finding the fixed points

Fixed points—and therefore unstable periodic orbits—may be determined by a slight adaptation of a typical algorithm for generating Poincaré sections.[3] One must keep track of pairs of consecutive points (θ_n,ω_n) and $(\theta_{n+1},\omega_{n+1})$, calculate the distance between them, and compare that distance to some predetermined small distance, ϵ. If the distance is less than ϵ then the coordinates indicate the presence of a nearby fixed point (θ_F,ω_F). Typically, the system will return to the neighborhood of the fixed point several times during a run and yield several closely spaced values for the fixed point. These must be averaged to obtain an estimate of the location of the nearby fixed point. Furthermore there are typically several fixed points from which to select. For our parameters we chose to stabilize the fixed point located at $\theta_F=1.523$, and $\omega_F=-0.415$. (In our case the Poincaré section is taken at the beginning of the forcing cycle.)

These procedures for finding fixed points can be modified to find period-2 or higher periodicity orbits. For period-k orbits one would simply check $(\theta_{n+k},\omega_{n+k})$ against (θ_n,ω_n). In general, control is easier for small values of k.

B. Effect of the parameter change

The next step is to determine how variation in the damping of the pendulum affects the coordinates of the fixed point. Near (θ_F,ω_F) a small change δq in the parameter q will result in a new fixed point (θ_F',ω_F') which can be approximated by

$$\begin{pmatrix}\theta_F'\\ \omega_F'\end{pmatrix}\approx\begin{pmatrix}\theta_F\\ \omega_F\end{pmatrix}+\delta q\begin{pmatrix}\partial\theta_F/\partial q\\ \partial\omega_F/\partial q\end{pmatrix}. \tag{3}$$

To determine the vector $(\partial\theta_F/\partial q,\partial\omega_F/\partial q)$ we simply make a small change in q and observe the change in fixed points while q is held constant at its new value. Figure 3 shows graphs of θ_F and ω_F vs q. Though there is some scatter a linear approximation near the fixed point suffices. The slopes are determined by a least-squares fit of the data. In this discussion we use

$$(\partial\theta_F/\partial_q,\partial\omega_F/\partial_q)=(-0.41,-0.29).$$

These slopes are uncertain by about ±0.06 and ±0.02, respectively. However, the control mechanism is not especially sensitive and variations of this magnitude seem to be tolerable.

C. The transformation, m

In general, the transformation m is a complicated nonlinear mapping of (θ_n,ω_n) onto $(\theta_{n+1},\omega_{n+1})$. However, in a small region of the phase plane the transformation can be approximated by a linear map. Near the fixed point this map may be written as

$$\begin{pmatrix}\theta_{n+1}\\ \omega_{n+1}\end{pmatrix}\approx\begin{pmatrix}\theta_n\\ \omega_n\end{pmatrix}+m\begin{pmatrix}\theta_n-\theta_F\\ \omega_n-\omega_F\end{pmatrix}, \tag{4}$$

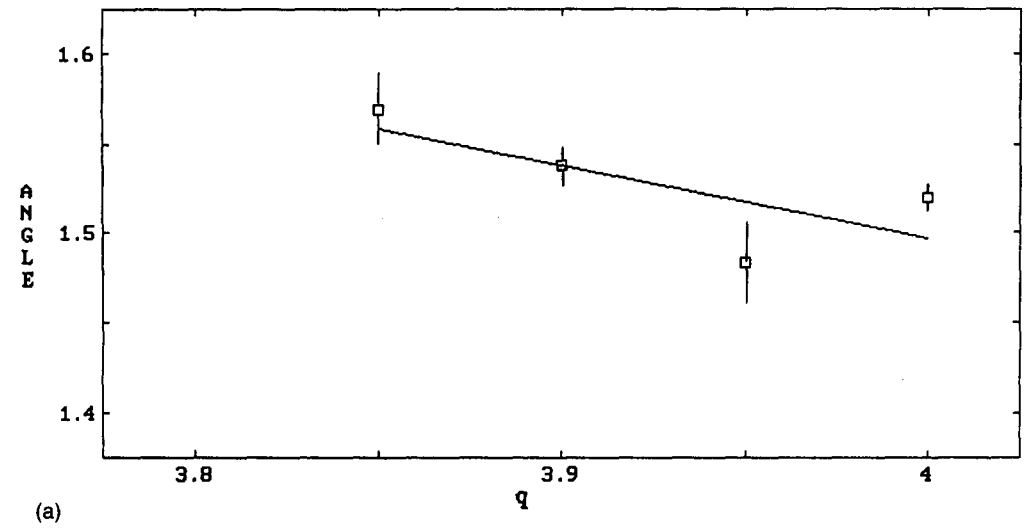

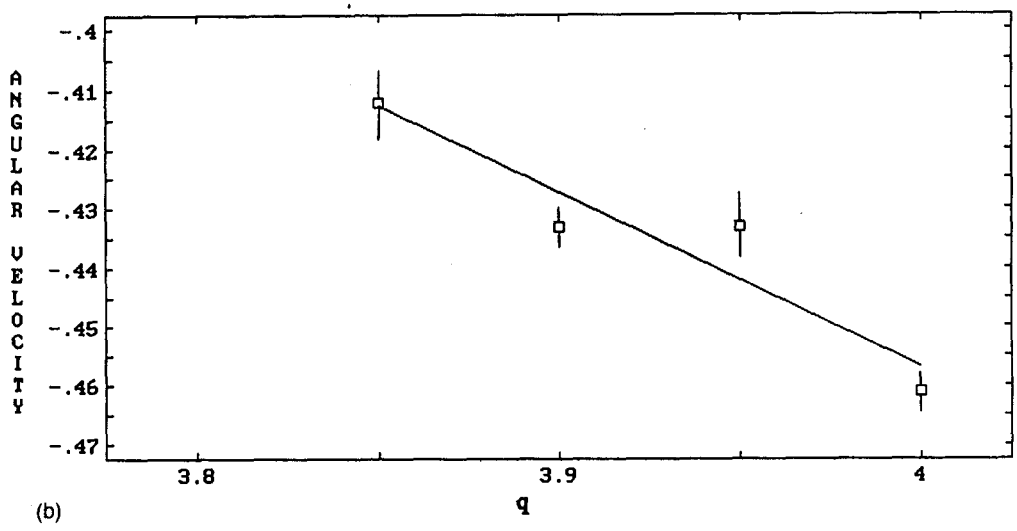

Fig. 3. Coordinates of the fixed point (of the Poincaré section) of an unstable periodic orbit are shown as a function of the friction parameter q. The straight line is a least-squares fit to the points. In (a) the fixed angle varies with q, and in (b) the fixed angular velocity varies with q.

where m is expressed as a 2 by 2 matrix:

$$m=\begin{pmatrix} m_{11} & m_{12} \\ m_{21} & m_{22} \end{pmatrix}. \tag{5}$$

We compress the notation by defining

$$\begin{pmatrix} \Delta\theta_n \\ \Delta\omega_n \end{pmatrix} \equiv \begin{pmatrix} \theta_n-\theta_F \\ \omega_n-\omega_F \end{pmatrix} \quad \text{and} \quad \begin{pmatrix} \Delta\theta_{n+1} \\ \Delta\omega_{n+1} \end{pmatrix} \equiv \begin{pmatrix} \theta_{n+1}-\theta_F \\ \omega_{n+1}-\omega_F \end{pmatrix}.$$

Therefore Eq. (1) can be written as

$$\begin{pmatrix} \Delta\theta_{n+1} \\ \Delta\omega_{n+1} \end{pmatrix} = m \begin{pmatrix} \Delta\theta_n \\ \Delta\omega_n \end{pmatrix}. \tag{6}$$

On the Poincaré surface there are special curves emanating from the fixed point (θ_F, ω_F): the *unstable manifold* along which successive points *leave* the fixed point, and the *stable manifold* along which successive points *approach* the fixed point. (A fixed point with these properties is said to be *hyperbolic*.) Near the fixed point, vectors that are already pointing along the stable or unstable manifolds keep their respective directions under the transformation m and therefore are *eigenvectors* of m. Solution of the corresponding eigenvalue problem yields the eigenvalues, λ_s and λ_u, and the respective eigenvectors, $\mathbf{e}_s$ and $\mathbf{e}_u$. Numerical values of these quantities are used in the control algorithm.

For an *experimental* dynamical system, determination of m requires many observations of the behavior of the system near the fixed point and a statistical averaging of that behavior. We adopt a simpler approach for our numerical simulation of the pendulum. The elements of m are found by following the evolution through one cycle of a pair of linearly independent vectors, near the fixed point. Our approach is to form initial pairs of vectors from pairs of perpendicular sides of the small box whose vertices are shown in Fig. 4. (The box encloses the unstable fixed point.) After one forcing cycle, the evolved pairs of points give new vectors that lie approximately along a straight line in Fig. 4. The matrix m determined from the evolution of these pairs of vectors is

$$m=\begin{pmatrix} -3.42 & -5.79 \\ -1.52 & -2.48 \end{pmatrix}. \tag{7}$$

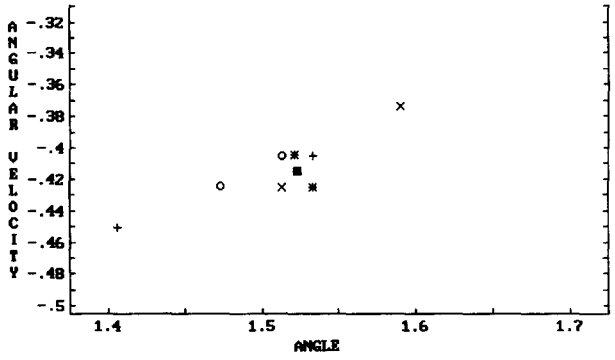

Fig. 4. Diagram showing the evolution of four points at the corners of a square through one forcing cycle. By treating pairs of points as evolving vectors in the (θ,ω) plane, the transformation matrix m is determined. The solid square is centered at (θ_F,ω_F). (If the unstable fixed point were determined exactly and the surrounding square was very small, then the fixed point would be centrally located among the transformed points.)

Solution of the eigenvalue problem associated with m yields the eigenvalues and eigenvectors

$$\lambda_u=-5.85, \quad \mathbf{e}_u=(e_{u1},e_{u2})=(0.92,0.40),$$
$$\lambda_s=+0.050, \quad \mathbf{e}_s=(e_{s1},e_{s2})=(0.86,-0.52). \tag{8}$$

(The eigenvectors are normalized to unity.)

For reasons that will shortly become evident we also calculate vectors $\mathbf{f}_u$ and $\mathbf{f}_s$ that are perpendicular to $\mathbf{e}_s$ and $\mathbf{e}_u$, respectively. This is achieved by using the relationships

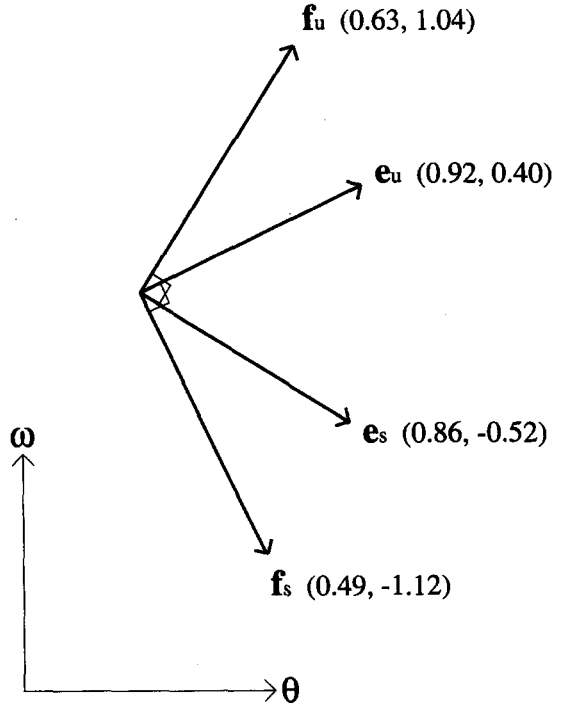

Fig. 5. An illustration of the calculated eigenvectors $\mathbf{e}_s$ and $\mathbf{e}_u$, and the corresponding orthogonal vectors, $\mathbf{f}_s$ and $\mathbf{f}_u$, in the (θ,ω) plane.

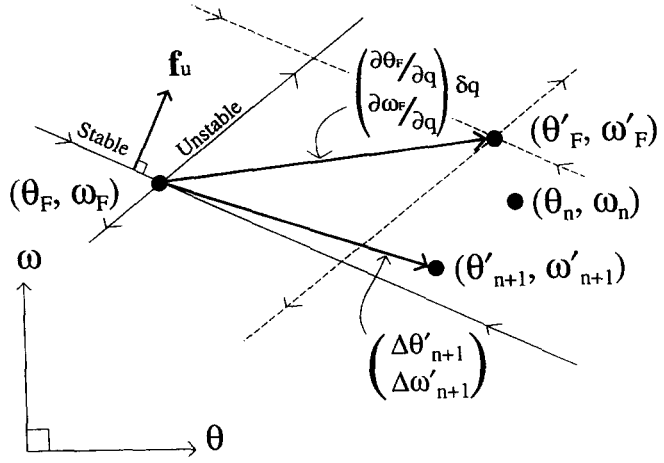

Fig. 6. A region of the (θ,ω) plane near the fixed point. The solid lines that intersect at (θ_F,ω_F) are the manifolds of the fixed point. Arrows pointing toward the fixed point mark the stable manifold and arrows pointing away from the fixed point mark the unstable manifold. The dashed lines that intersect at (θ'_F,ω'_F) represent the analogous configuration after a change of δq in the friction parameter. The control mechanism forces the $(n+1)$ point toward the stable manifold of (θ_F,ω_F).

$$\mathbf{f}_u\cdot\mathbf{e}_s=0 \quad \text{and} \quad \mathbf{f}_s\cdot\mathbf{e}_u=0,$$

and, for normalization, we let

$$\mathbf{f}_u\cdot\mathbf{e}_u=1 \quad \text{and} \quad \mathbf{f}_s\cdot\mathbf{e}_s=1.$$

The various directions and magnitudes of all these vectors are indicated in Fig. 5. In our case

$$\mathbf{f}_u=(f_{u1},f_{u2})=(0.63,1.04), \quad \text{and}$$
$$\mathbf{f}_s=(f_{s1},f_{s2})=(0.49,-1.12).$$

Finally, the derivation of the control algorithm will use the fact that the map m can be written as a combination of the above quantities:

$$m=\lambda_u\begin{pmatrix}e_{u1}\\e_{u2}\end{pmatrix}(f_{u1}\ f_{u2})+\lambda_s\begin{pmatrix}e_{s1}\\e_{s2}\end{pmatrix}(f_{s1}\ f_{s2}). \tag{9}$$

(See the Appendix for a derivation of this expression.)

IV. THE CONTROL ALGORITHM

The goal of the control mechanism is to force the pendulum's trajectory toward the fixed point on the Poincaré section. This is achieved by adjusting the friction parameter q so as to push the intersection point of the trajectory with the Poincaré section onto the stable manifold near the fixed point. Then the natural attraction along the stable manifold will pull the intersection point to the fixed point.

Let us begin with the schematic illustration of the Poincaré section near the fixed point as shown in Fig. 6. The fixed point (θ_F,ω_F) is located at the intersection of the stable and unstable manifolds. If q is changed by an amount δq, then the fixed point is moved to a new position (θ'_F,ω'_F) such that

$$\begin{pmatrix}\theta'_F\\\omega'_F\end{pmatrix}=\begin{pmatrix}\theta_F\\\omega_F\end{pmatrix}+\delta q\begin{pmatrix}\partial\theta_F/\partial q\\\partial\omega_F/\partial q\end{pmatrix}. \tag{10}$$

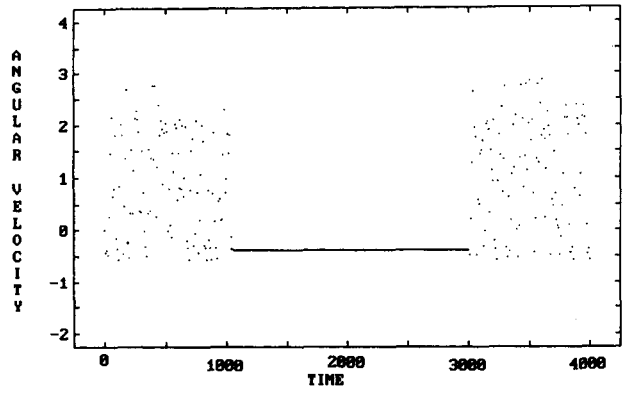

Fig. 7. A graph of angular velocity at the beginning of each forcing cycle as a function of time. Control is initiated at $t=1000$ and released at $t=3000$.

With the changed q the next point $(\theta'_{n+1},\omega'_{n+1})$ becomes

$$\begin{pmatrix}\theta'_{n+1}\\ \omega'_{n+1}\end{pmatrix}=\begin{pmatrix}\theta'_F\\ \omega'_F\end{pmatrix}+m\begin{pmatrix}\Delta'\theta_n\\ \Delta'\omega_n\end{pmatrix}\quad\text{where}$$

$$\begin{pmatrix}\Delta'\theta_n\\ \Delta'\omega_n\end{pmatrix}=\begin{pmatrix}\theta_n-\theta'_F\\ \omega_n-\omega'_F\end{pmatrix}. \tag{11}$$

We assume that m is roughly constant for small δq. [The primes denote quantities referred to the new fixed point (θ'_F,ω'_F).] This new point $(\theta'_{n+1},\omega'_{n+1})$ is the result of the map m with $q+\delta q$ acting on (θ_n,ω_n). We denote the vector from the original fixed point (θ_F,ω_F) to the new point as

$$\begin{pmatrix}\Delta\theta'_{n+1}\\ \Delta\omega'_{n+1}\end{pmatrix}=\begin{pmatrix}\theta'_{n+1}-\theta_F\\ \omega'_{n+1}-\omega_F\end{pmatrix}. \tag{12}$$

Finally, by including the change δq in the damping and the effect of the map m, the vector of Eq. (12) may be written first as

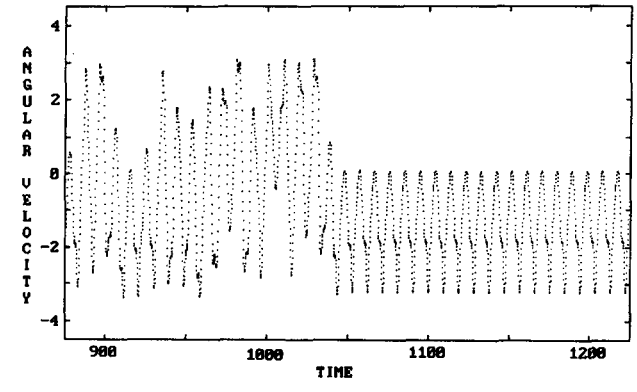

Fig. 8. A time series of the angular velocity shown near the initiation of control at $t=1000$. In contrast to Fig. 7, which only shows the angular velocity once per forcing cycle, this figure gives the complete sequence of angular velocity values. Complete control emerges after several cycles.

$$\begin{pmatrix}\Delta\theta'_{n+1}\\ \Delta\omega'_{n+1}\end{pmatrix}=\begin{pmatrix}\theta'_F\\ \omega'_F\end{pmatrix}-\begin{pmatrix}\theta_F\\ \omega_F\end{pmatrix}+m\begin{pmatrix}\theta_n-\theta'_F\\ \omega_n-\omega'_F\end{pmatrix}$$

and then as

$$\begin{pmatrix}\Delta\theta'_{n+1}\\ \Delta\omega'_{n+1}\end{pmatrix}=\begin{pmatrix}\partial\theta_F/\partial q\\ \partial\omega_F/\partial q\end{pmatrix}\delta q+m\left[\begin{pmatrix}\Delta\theta_n\\ \Delta\omega_n\end{pmatrix}-\begin{pmatrix}\partial\theta_F/\partial q\\ \partial\omega_F/\partial q\end{pmatrix}\delta q\right]. \tag{13}$$

Using m in the expanded form of Eq. (6) this vector may be written as

$$\begin{pmatrix}\Delta\theta'_{n+1}\\ \Delta\omega'_{n+1}\end{pmatrix}=\begin{pmatrix}\dfrac{\partial\theta_F}{\partial q}\\ \dfrac{\partial\omega_F}{\partial q}\end{pmatrix}\delta q+\left[\lambda_u\begin{pmatrix}e_{u1}\\ e_{u2}\end{pmatrix}(f_{u1}\ f_{u2})\right.$$
$$\left.+\lambda_s\begin{pmatrix}e_{s1}\\ e_{s2}\end{pmatrix}(f_{s1}\ f_{s2})\right]\left[\begin{pmatrix}\Delta\theta_n\\ \Delta\omega_n\end{pmatrix}-\delta q\begin{pmatrix}\dfrac{\partial\theta_F}{\partial q}\\ \dfrac{\partial\omega_F}{\partial q}\end{pmatrix}\right]. \tag{14}$$

For control we want the point $(\theta'_{n+1},\omega'_{n+1})$ to move toward the stable manifold and therefore the vector $(\Delta\theta'_{n+1},\Delta\omega'_{n+1})$ should move toward alignment with the stable manifold. This means that δq should be adjusted to make the dot product of the vectors $(\Delta\theta'_{n+1},\Delta\omega'_{n+1})$ and $\mathbf{f}_u$ equal to zero:

$$(f_{u1}\ f_{u2})\begin{pmatrix}\Delta\theta'_{n+1}\\ \Delta\omega'_{n+1}\end{pmatrix}=0. \tag{15}$$

When combined with Eq. (14) this condition leads to the OGY result,

$$\delta q=\frac{\lambda_u}{(\lambda_u-1)}\cdot\frac{(f_{u1}\ f_{u2})\begin{pmatrix}\Delta\theta_n\\ \Delta\omega_n\end{pmatrix}}{(f_{u1}\ f_{u2})\begin{pmatrix}\partial\theta/\partial q\\ \partial\omega/\partial q\end{pmatrix}}. \tag{16}$$

This expression gives the change in q that is necessary to modify the trajectory so that its next intersection with the Poincaré section is close to the stable manifold of (θ_F,ω_F). It is this expression that is used to vary q for each Poincaré cycle.

The control method is applied to a numerical simulation of the pendulum as modeled by Eq. (1). Results are shown in Fig. 7 where the angular velocity ω at the beginning of each cycle is plotted as a function of time. Control is initiated at $t=1000$ and turned off at $t=3000$. Before and after these times the motion is clearly chaotic. During the control epoch the orbit returns to (θ_F,ω_F) and the pendulum has been stabilized to a period-1 motion.

When control is initiated the orbit takes a little time to achieve stability. The reason for this delay is as follows. Typically, only small changes in the parameter q are allowed since large changes might push the system into a completely different dynamical state. If δq^* is the maximum allowed change then this equation also provides an estimate of the maximum allowed distance of the point (θ_n,ω_n) from the fixed point (θ_F,ω_F). Therefore the fact that the control region may be fairly small means there will be a delay from the time control is activated until the point on the Poincaré

section arrives within the control region. A quantitative measure of this effect is provided in the original paper of Ott *et al.*[13] Figure 8 is a time series of the angular velocity that shows the implementation of the control on a finer time scale. Control is initiated at $t=1000$ but several forcing cycles are required to achieve full control of the pendulum's motion. In this case the control radius, $\|(\Delta\theta_n, \Delta\omega_n)\| \sim 0.3$ and $\delta q^* \sim 0.1$.

Finally we note that the values of the numbers in the matrix m used for the control algorithm need not be especially precise. Control was often achieved even when some of the numbers were different from the values quoted above by several percent. The method seems to be remarkably robust and, given the small values of δq, quite efficient.

V. CONCLUSION

We have shown how the OGY method of control can be applied to a classical physical model, the driven pendulum. Many details of the calculation have been provided to make the process more accessible to nonspecialists.

ACKNOWLEDGMENTS

I would like to thank Jerry P. Gollub and the reviewers for many detailed and helpful suggestions for improvement of this paper.

APPENDIX: A SIMPLE DERIVATION OF THE EXPANSION OF m IN TERMS OF λ_u, λ_s, $\mathbf{e}_u$, $\mathbf{e}_s$, $\mathbf{f}_u$, and $\mathbf{f}_s$

Consider the expression

$$m\left[\begin{pmatrix} e_{u1} \\ e_{u2} \end{pmatrix} + \begin{pmatrix} e_{s1} \\ e_{s2} \end{pmatrix}\right] = \lambda_u \begin{pmatrix} e_{u1} \\ e_{u2} \end{pmatrix} + \lambda_s \begin{pmatrix} e_{s1} \\ e_{s2} \end{pmatrix} = \lambda_u \begin{pmatrix} e_{u1} \\ e_{u2} \end{pmatrix} (\mathbf{f}_u \cdot \mathbf{e}_u + \mathbf{f}_u \cdot \mathbf{e}_s) + \lambda_s \begin{pmatrix} e_{s1} \\ e_{s2} \end{pmatrix} (\mathbf{f}_s \cdot \mathbf{e}_s + \mathbf{f}_s \cdot \mathbf{e}_u),$$

where we use the fact that

$$\mathbf{f}_u \cdot \mathbf{e}_u = 1 = \mathbf{f}_s \cdot \mathbf{e}_s \quad \text{and} \quad \mathbf{f}_u \cdot \mathbf{e}_s = 0 = \mathbf{f}_s \cdot \mathbf{e}_u .$$

Then

$$m[\mathbf{e}_u + \mathbf{e}_s] = \left[\lambda_u \begin{pmatrix} e_{u1} \\ e_{u2} \end{pmatrix} \mathbf{f}_u + \lambda_s \begin{pmatrix} e_{s1} \\ e_{s2} \end{pmatrix} \mathbf{f}_s\right] \cdot (\mathbf{e}_u + \mathbf{e}_s).$$

Finally, the matrix inside the square brackets may be expanded in component form as

$$m = \lambda_u \begin{pmatrix} e_{u1} \\ e_{u2} \end{pmatrix} (f_{u1} \;\; f_{u2}) + \lambda_s \begin{pmatrix} e_{s1} \\ e_{s2} \end{pmatrix} (f_{s1} \;\; f_{s2}).$$

[1] R. Dugas, *Mechanics in the 17th Century* (Central Book, New York, 1958), p. 76.

[2] J. A. Blackburn, S. Vik, Wu Binru, and H. J. T. Smith, "Driven Pendulum for studying chaos," Rev. Sci. Instrum. **60**, 422–436 (1989).

[3] G. L. Baker and J. P. Gollub, *Chaotic Dynamics: An Introduction* (Cambridge University Press, Cambridge, 1990), Chap. 3.

[4] D. D'Humieres, M. R. Beasley, B. A. Huberman, and A. Libchaber, "Chaotic states and routes to chaos in the forced pendulum," Phys. Rev. A **26**, 3483–96 (1982); E. G. Gwinn and R. M. Westervelt, "Fractal basin boundaries and intermittency in the driven damped pendulum," *ibid.* **33**, 4143–55 (1986).

[5] L. Page, *Introduction to Theoretical Physics* (Van Nostrand, New York, 1928); H. Goldstein, *Classical Mechanics* (Addison-Wesley, Reading, MA, 1980), 2nd ed.

[6] R. C. Hilborn, *Chaos and Nonlinear Dynamics* (Oxford University Press, New York, 1994).

[7] F. C. Moon, *Chaotic and Fractal Dynamics, An introduction for Applied Scientists and Engineers* (Wiley, New York, 1992).

[8] See, for example, the references in C. Chen and I. J. Haas, *Elements of Control Systems Analysis: Classical and Modern Approaches* (Prentice-Hall, Englewood Cliffs, NJ, 1968).

[9] W. L. Ditto and L. M. Pecora, "Mastering chaos," Sci. Am. August 78–84 (1993).

[10] R. W. Rollins, P. Parmananda, and P. Sherard, "Controlling chaos in highly dissipative systems: a simple recursive algorithm," Phys. Rev. E **47**, R780–R783 (1993).

[11] Z. Gills, C. Iwata, R. Roy, I. Schwartz, and I. Triandaf, "Tracking steady states: extending the stability regime of a multimode laser system," Phys. Rev. Lett. **69**, 3169–3172 (1992)

[12] I. B. Schwartz and I. Triandaf, "Control and prediction in seasonally driven population models," in *Predictability and Nonlinear Modelling in Natural Sciences and Economics*, edited by J. Grasman and G. Van Straten (Kluwer, Dordrecht, 1994).

[13] E. Ott, C. Grebogi, and J. A. Yorke, "Controlling chaos," Phys. Rev. Lett. **64**, 1196–1199 (1990).

[14] W. L. Ditto, S. N. Rauseo, and M. L. Spano, "Experimental control of chaos," Phys. Rev. Lett. **65**, 3211–3214 (1990).

[15] J. Starrett and R. Tagg, "Control of a chaotic parametrically driven pendulum," Phys. Rev. Lett. **74**, 1974–77 (1995).

[16] G. Nitsche and U. Dressler, "Controlling chaotic dynamical systems using time delay coordinates," Physica D **58**, 153–164 (1992).

[17] B. Hubinger, R. Doerner, and W. Martienssen, "Local control of chaotic motion," Z. Phys. B **90**, 103–106 (1993).

TORTUOUS PROSE

What is most disturbing about the "learned journalese"—the unnecessarily tortuous prose which still survives in most scientific journals—is that its perpetrators are scarcely aware of their abuse of the language. Like a young child who becomes bilingual by daily contact with parents speaking two languages, many scientists never even consider the contrast between their conversation over the breakfast table and the weird, stilted cadences they use to communicate with their peers. Translate one into the other and the problem becomes obvious: "It has been shown by the present author, on the basis of preliminary evidence that has not yet been independently replicated by other investigators, that an appropriate quantity of milk is absent from the refrigerator."

Bernard Dixon, "Plain words, please," New Scientist **137** (1865), 39 (20 March 1993).